ANISOTROPY IN FAST AND SLOW SOLAR WIND FLUCTUATIONS

S. DASSO[1]

Instituto de Astronomía y Física del Espacio and Departamento de Física, Facultad de Ciencias Exactas y Naturales, Universidad de Buenos Aires,
C.C. 67, Sucursal 28, 1428 Buenos Aires, Argentina; sdasso@iafe.uba.ar

L. J. MILANO AND W. H. MATTHAEUS

Bartol Research Institute, University of Delaware, 217 Sharp Lab, Newark, DE 19716; lmilano@udel.edu, yswhm@udel.edu

AND

C. W. SMITH

Institute for the Study of Earth, Oceans, and Space, University of New Hampshire, Morse Hall,
39 College Road, Durham, NH 03824; Charles.Smith@unh.edu

Received 2005 April 8; accepted 2005 November 11; published 2005 December 13

ABSTRACT

Using 5 years of spacecraft data from near Earth orbit, we investigate the correlation anisotropy of solar wind magnetohydrodynamic-scale fluctuations and show that the nature of the anisotropy differs in fast (>500 km s^{-1}) and slow (<400 km s^{-1}) streams. In particular, fast streams are relatively more dominated by fluctuations with wavevectors quasi-parallel to the local magnetic field, while slow streams, which appear to be more fully evolved turbulence, are more dominated by quasi-perpendicular fluctuation wavevectors.

Subject headings: MHD — plasmas — solar wind — turbulence — waves

A distinctive feature of plasma turbulence in the magneto-hydrodynamic (MHD) regime is its tendency to develop and sustain anisotropy relative to the direction of the large-scale magnetic field. The significance of this preferred direction has repeatedly emerged in experimental (Robinson & Rusbridge 1971), observational (Matthaeus et al. 1990), theoretical (Montgomery et al. 1972), and numerical (Milano et al. 2001) studies. Anisotropy properties in solar wind turbulence have been observed in situ for almost 40 years, providing important connections to anisotropy in MHD theory, as well as having impact on heliospheric plasma dynamics, transport, and scattering. Here we examine the correlation anisotropy of solar wind turbulence at 1 AU using 5 years of data from the *ACE* spacecraft. We focus on statistical differences in anisotropy that occur in fast- and slow-speed samples of solar wind.

Two paradigms have emerged from decades of analysis of solar wind turbulence. Fluctuations may be described either as noninteracting Alfvén waves propagating away from sources near the Sun (Belcher & Davis 1971) or as an active, evolving turbulent medium, displaying properties similar to Kolmogorov hydrodynamic turbulence (see Tu & Marsch 1995 and references therein). Although wave and turbulence descriptions appear to be very different, it is likely that elements of each picture enter into describing the solar wind, since it is expected that MHD turbulence in its various regimes involves a balance of propagation and nonlinear effects (Zhou et al. 2004). The degree and type of anisotropy have direct implications for the wave/turbulence dichotomy.

For spatially uniform, nearly incompressible turbulence with an applied DC magnetic field, spectral transfer is predominantly toward higher perpendicular wavenumber (steeper perpendicular gradients). To the extent that parallel wavenumbers are unchanged, the (Alfvén) wave frequency remains constant or nearly constant, while the cascade pushes energy toward smaller (perpendicular) wavelength. For driving or initial conditions confined to moderate or low parallel wavenumber, this scenario leads to highly anisotropic, low-frequency, nearly in-compressible, quasi–two-dimensional turbulence. However, there are other factors that can influence turbulence anisotropy (cascade of compressive fluctuations tends to be isotropic, wave-particle interactions can inject fluctuations at relatively high parallel wavenumbers of the order of the resonant proton gyroradius, etc.).

Of the various descriptions of anisotropic wave and turbulence properties of the solar wind, the so-called Maltese cross (Matthaeus et al. 1990) is one that illustrates the clear implication that no simple symmetry such as one-dimensional "slab" or two-dimensional or quasi–two-dimensional turbulence or "structures" is sufficient to characterize all of the observed MHD-scale fluctuations. In particular, level contours of the magnetic self-correlation are seen to have a crosslike pattern when plotted in a two-dimensional plane in which one of the axes is parallel to the magnetic field. There is a lobe along each axis. A suggestive but oversimplified interpretation is the presence of two components: slablike fluctuations, with mainly parallel wavevectors, and fluctuations of quasi–two-dimensional nature, having mainly perpendicular wavevectors. These simplified ingredients provide a useful kinematic parameterization. Despite the superficial implication that the two ingredients are completely distinct, a number of studies indicate that wavelike fluctuations and those of the quasi–two-dimensional turbulence type cannot evolve independently (e.g., Ghosh et al. 1998a, 1998b; Goldstein et al. 2003). Moreover, a recent observational study (Milano et al. 2004) has shown that the normalized cross-helicity content does not depend significantly on the angle between the wavenumber direction and the mean magnetic field.

If correct, the paradigm of the Maltese cross spectrum and, through further idealization, two-component models are useful in providing a detailed picture of anisotropy, and they also afford economy in calculations. However, the empirical extraction of the Maltese cross requires the use of a large number of data samples, and therefore crucial questions arise regarding its interpretation. Is this pattern representative of physical properties of individual samples? Or is it a superposition effect of distinctly characterized populations? Are there systematic cor-

---

[1] Member of the Carrera del Investigador Científico, CONICET, Argentina.

relations that are hidden in the methodology for obtaining it? It may be difficult to address all such concerns immediately, but the issue of systematic effects associated with solar wind speed is one that arises with high priority. Wind speed enters into the analysis procedure in two important ways, both owing, to one degree or another, to the use of single-spacecraft observations: First, we use the familiar frozen-in approximation, which allows conversion of time lags into spatial lags in the correlation analysis. Second, we are interested in correlations relative to the local mean magnetic field, and given that we mainly use 1 AU observations, the variation of the mean field is associated with varying solar wind speed.

Various features of the solar wind plasma are speed related and related to stream structure, which is inherently organized by latitude and speed. The relative abundance of charge states of heavy ions is different in fast and slow wind: low values of charge state are generally associated with higher speed streams (e.g., Zurbuchen et al. 2002 and references therein). Charge state abundance also varies with magnetic topology, as deduced from in situ observations in the interplanetary medium (see, e.g., Henke et al. 1998); these authors have shown that faster interplanetary coronal mass ejections that are magnetic clouds contain a charge state composition similar to that of slow solar wind. Therefore the wind speed, the charge state distribution, and the magnetic topology are three candidates for introducing systematic effects in the Maltese cross analysis and interpretation. We focus here on one of these, the wind speed.

We analyze ~5 years' observations of proton densities and magnetic and bulk velocity fields, measured by MAG (the Magnetic Field Instrument; Smith et al. 1998) and the Solar Wind Electron, Proton, and Alpha Monitor (SWEPAM; McComas et al. 1998), aboard the *Advanced Composition Explorer* (*ACE*) spacecraft, from 1998 February 10 to 2002 December 5. The data have been analyzed with a cadence of 1 minute, and they have typical uncertainties of about 0.1 nT for the magnetic field, ~1% for the bulk velocity, and ~15% for the proton density. The solar wind observations we analyze here correspond to a distance of ~1 AU from the Sun and are essentially on the ecliptic plane. The 1 minute data points are grouped in 2 day intervals, yielding N subseries (intervals). We then shift our data set by 1 day and repeat the procedure, thus maximizing the data utilization. Intervals that show sector crossings and large gradients in the heliocentric radial velocity profile are identified by visual inspection and removed. The final number of analyzed intervals is $N = 992$. For each interval I ($I = 1$, ..., N), using the observed magnetic ($\boldsymbol{B}^I$) and velocity ($\boldsymbol{V}^I$) fields, we define the fluctuation fields $\boldsymbol{b}^I$ and $\boldsymbol{v}^I$, and the Elsässer variables $\boldsymbol{z}^{I,\pm} = \boldsymbol{v}^I \pm \boldsymbol{b}^I$, as follows:

$$\boldsymbol{v}^I = \boldsymbol{V}^I - \boldsymbol{U}_0^I, \qquad \boldsymbol{b}^I = \boldsymbol{B}^I - \boldsymbol{B}_0^I. \qquad (1)$$

where $\boldsymbol{U}_0^I$ and $\boldsymbol{B}_0^I$ denote linear fits to $\boldsymbol{V}$ and $\boldsymbol{B}$ (respectively) in the interval I, intended to remove coherent trends in the data (Matthaeus & Goldstein 1982). Magnetic fields are in velocity units: $\boldsymbol{B}^I \rightarrow \boldsymbol{B}^I/(4\pi\rho^I)^{1/2}$, using the mean mass density for the interval I (ρ_I).

Our main goal is to compute two-point correlations of the form

$$R_{vv}(\boldsymbol{r}) = \langle \boldsymbol{v}(\boldsymbol{x}) \cdot \boldsymbol{v}(\boldsymbol{x} + \boldsymbol{r}) \rangle. \qquad (2)$$

Analogous definitions hold for R_{bb} and R_{vb}, and for the correlations in the Elsässer variables, R_{++} and R_{--}. Note that equation (2) is the trace of the usual two-point correlation tensor

for the velocity field. The single-spacecraft *ACE* data that we employ provide two-time single-point correlations. However, because of the super-Alfvénic and supersonic character of the solar wind, we construct spatial correlation functions in the usual way (Matthaeus & Goldstein 1982) by making use of the MHD analogs of the Taylor "frozen-in flow" hypothesis (Taylor 1938). For a given interval I, the mean solar wind velocity $\boldsymbol{V}_{sw}^I \equiv \langle \boldsymbol{V}^I \rangle$ gives the associated spatial lag $\boldsymbol{r} = t\boldsymbol{V}_{sw}^I$ at time t; this is assumed, with minimal error, to lie along the heliocentric radial direction. In this way we employ a "Blackman-Tukey" technique (Blackman & Tukey 1958) to compute the correlation functions $R^I(r)$, in the same way as done in Milano et al. (2004). We choose the maximum computed lag as $t_{max} = 16$ hr (so for a given interval I, the maximum spatial lag corresponds to $r_{max}^I = t_{max}|\boldsymbol{V}_{sw}^I|$). The computed $R^I(r)$ is windowed using a 10% cosine taper (Matthaeus & Goldstein 1982), and we complete $R^I(r)$ with zeros from r_{max}^I to the maximum spatial lag for the full set of analyzed intervals.

In order to compute statistics from the observed data, we normalize the fluctuating fields so that the fluctuation amplitudes in different intervals are comparable. We use a variance-based normalization scheme (e.g., Milano et al. 2004) and compute, in each data interval, normalized correlation functions of the form $R_{fg}^{norm,I}(r) \equiv \lambda^I \langle \boldsymbol{f}^I(\boldsymbol{x}) \cdot \boldsymbol{g}^I(\boldsymbol{x} + \boldsymbol{r}) \rangle$, where $\lambda^I \equiv \langle \boldsymbol{f} \cdot \boldsymbol{g} \rangle / \langle \boldsymbol{f}^I \cdot \boldsymbol{g}^I \rangle$ and $\boldsymbol{f}$ and $\boldsymbol{g}$ represent any of the fluctuating fields defined above. Note that the chosen normalization implies that $R_{fg}^{norm,I}(0) = \langle \boldsymbol{f} \cdot \boldsymbol{g} \rangle$ for all intervals I. For simplicity of notation, we omit the "norm" label hereafter. The typical shape of the averaged $R^{norm}(r)$ obtained from this procedure, as well as its typical uncertainty (error bars), is reported in Figures 1 and 2 of Milano et al. (2004).

In order to analyze the anisotropy of the fluctuations while distinguishing the slow from the fast solar wind, we label each interval according to $|\boldsymbol{V}_{sw}^I|$ and the value of the angle θ^I between the direction of the mean field $\boldsymbol{V}_A^I \equiv \langle \boldsymbol{B}^I \rangle$ and $\boldsymbol{V}_{sw}^I$. We then analyze variations in several statistical quantities as a function of θ and $|\boldsymbol{V}_{sw}|$. Here we define five ranges for θ: $0° \leq \theta_1 < 25°$, $25° \leq \theta_2 < 40°$, $40° \leq \theta_3 < 50°$, $50° \leq \theta_4 < 65°$, and $65° \leq \theta_5 < 90°$. We use two ranges for the solar wind velocity: "slow" solar wind, such that $|\boldsymbol{V}_{sw}^I| < 400$ km s^{-1} (364 intervals), and "fast" solar wind, such that $|\boldsymbol{V}_{sw}^I| > 500$ km s^{-1} (172 intervals). We exclude the middle range of velocities to enable a clearer distinction between the sets.

From the correlation functions of every interval, $R^I(r)$, we carry out conditional averages considering only those intervals that correspond to a given range of θ-values (θ_J being the center of each range, with $J = 1–5$) and to the different solar wind velocities (fast and slow solar wind, f and s, respectively), obtaining $R(r)_{f,\theta_J}$ and $R(r)_{s,\theta_J}$. For analysis of anisotropy, we project the inferred spatial separation (radial, as it emerges from a frozen-in flow) onto a two-dimensional plane spanned by a separation coordinate $r_\parallel$ parallel to the local mean magnetic field and a complementary perpendicular coordinate. Note that we are assuming axisymmetry about the mean magnetic field direction, as in Matthaeus et al. (1990). We then transform $(r, \theta_J) \rightarrow (r_\parallel, r_\perp)$, where $r_\parallel = r \cos \theta_J$ and $r_\perp = r \sin \theta_J$. In this way we deduce estimates for two (slow and fast) mean correlation functions: $R_s(r_\parallel, r_\perp)$ and $R_f(r_\parallel, r_\perp)$.

To give physical meaning to our analysis, we have grouped the fluctuations according to whether their $\langle \boldsymbol{v} \cdot \boldsymbol{b} \rangle$ correlation suggests propagation outward from the Sun ("out") or toward the Sun ("in") and consistently relabeled the Elsässer variables as z_{out} and z_{in} in each interval.
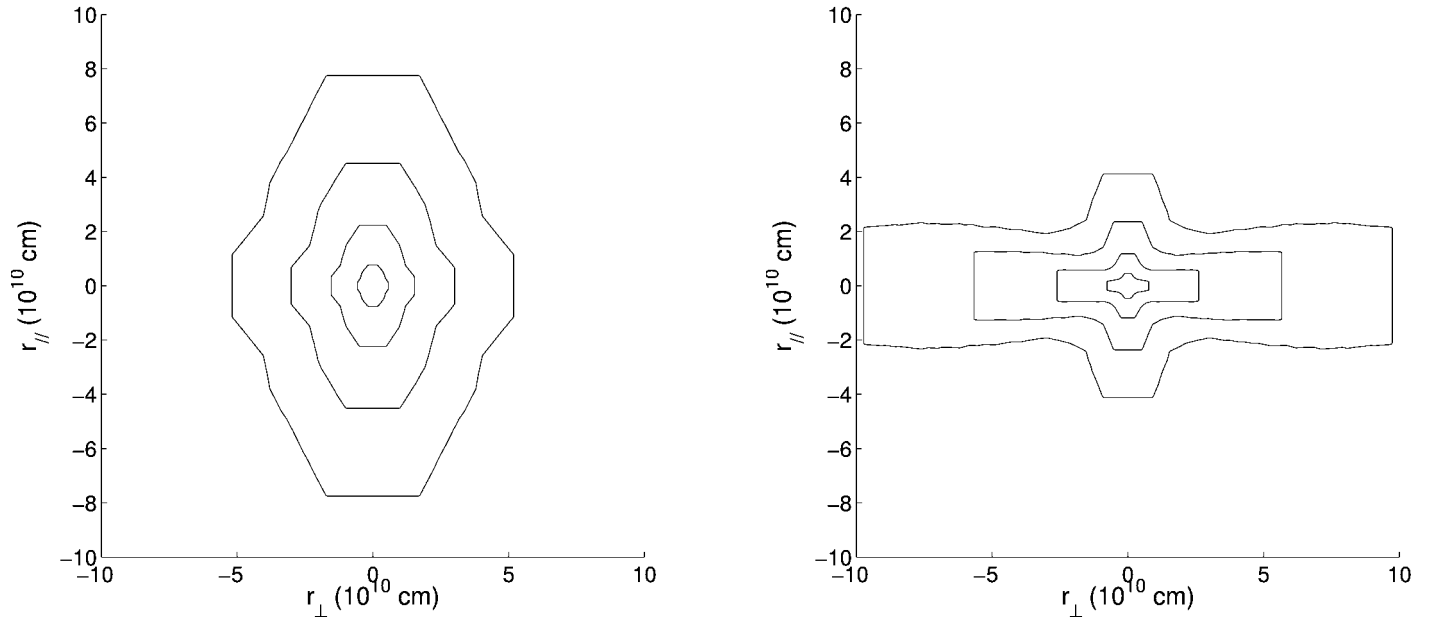
FIG. 1.—Level contours for $R_{bb}(\textbf{r})$. *Left*, slow solar wind ($V_{sw} < 400$ km s^{-1}); *right*, fast solar wind ($V_{sw} > 500$ km s^{-1}). (See text.) Levels are at 1200, 1400, 1600, and 1800 km^2 s^{-2}.

Figure 1 shows the cumulative ($\sim$5 yr) contour levels for slow and fast $R_{bb}(r_\parallel, r_\perp)$. Contours are plotted at the same values for slow wind ($V_{sw} < 400$ km s^{-1}) and for fast wind ($V_{sw} > 500$ km s^{-1}), which are shown in the left and right panels, respectively. It seems apparent from this figure that the slow wind shows a preference for perpendicular wavenumbers in the fluctuations, and that the fast solar wind fluctuations are biased into the parallel direction; $R_{vb} = (R_{out} - R_{in})/4$ (see Fig. 2), R_{vv}, R_{out}, and R_{in} (not shown here, for brevity) present qualitatively the same preference in the ($r_\parallel$, $r_\perp$)-plane. The relative errors for the average R_{bb}, R_{vv}, R_{out}, and R_{in}, at the correlation length, are $\sim$8% for the fast wind and $\sim$6% for the slow wind. R_{vb} presents a lower relative error ($\sim$3% for both kinds of solar wind).

A measure of anisotropy was suggested in Milano et al. (2001). The ratio of perpendicular to parallel second-order structure functions gives a measure of the ratio (squared) of Taylor microscales in these directions (in the limit where the separation tends to zero):

$$\Gamma = \lim_{l \to 0} [S(l_\perp)/S(l_\parallel)]. \qquad (3)$$

This definition corresponds to $\Gamma = (\lambda_\parallel^T/\lambda_\perp^T)^2$. In Table 1, we show an estimate of Γ in both the fast and slow solar wind. As a reference value, $\Gamma = 1$ obviously means isotropy. The values of Γ depart consistently from unity in the same sense
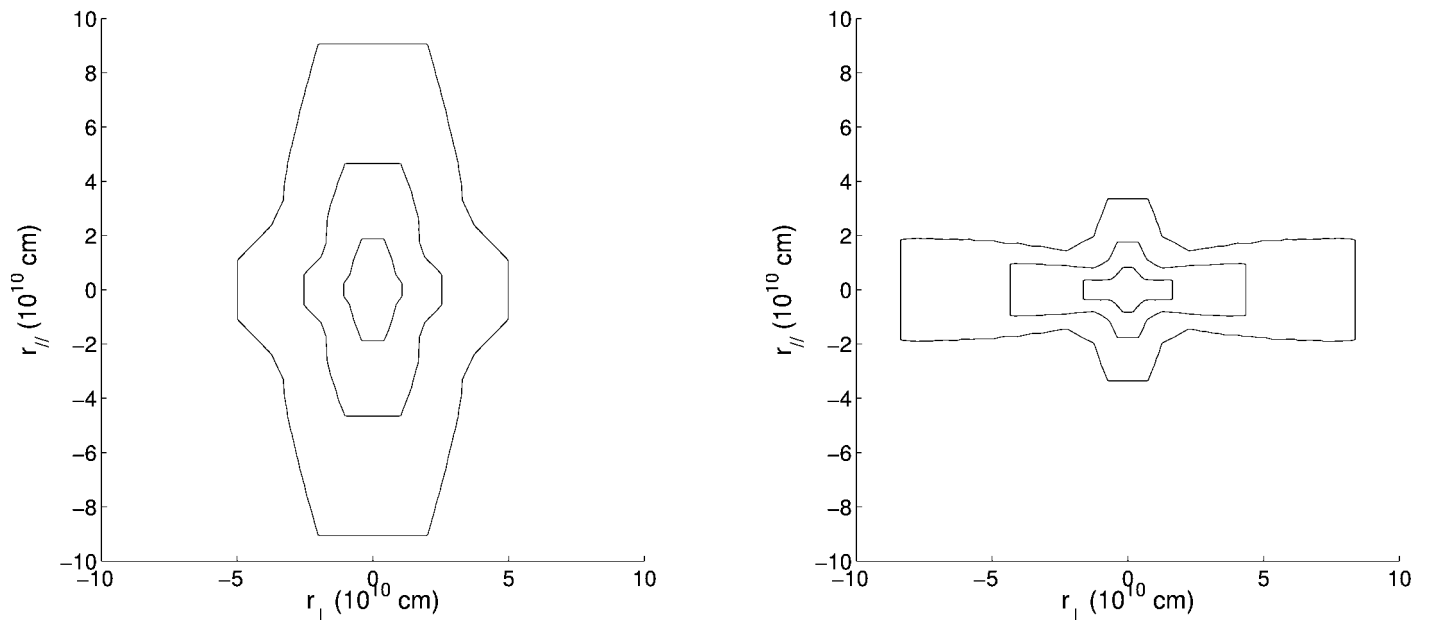

FIG. 2.—Same as Fig. 1, but for $R_{vb}(\textbf{r})$. Levels are at 425, 525, and 625 km^2 s^{-2}.

TABLE 1
ESTIMATE OF $\Gamma = (\lambda_\parallel^{\mathrm{T}}/\lambda_\perp^{\mathrm{T}})^2$: SQUARED RATIO
OF TAYLOR MICROSCALES

Wind	R_{bb}	R_{vv}	R_{out}	R_{in}	R_{vb}
Slow	1.4	1.3	3.1	1.6	4.1
Fast	0.6	0.5	0.6	0.4	0.6

TABLE 2
ESTIMATE OF $(\lambda_\parallel^{\mathrm{corr}}/\lambda_\perp^{\mathrm{corr}})^2$: SQUARED RATIO
OF CORRELATION SCALES

Wind	R_{bb}	R_{vv}	R_{out}	R_{in}	R_{vb}
Slow	1.4	1.1	1.4	1.1	1.7
Fast	0.5	0.4	0.5	0.8	0.4

as shown in Figures 1–2. The estimates are obtained by using the simple relationship

$$S(\boldsymbol{l})/2 = R(0) - R(\boldsymbol{l}). \qquad (4)$$

We evaluate l at the minimum finite possible separation in each case.

Finally, a comparison of the correlation lengths in the parallel and perpendicular directions is presented in Table 2. Correlation lengths, $\lambda^{\mathrm{corr}} = \int_0^\infty R(r)dr/R(0)$, are estimated as the values of r where the decreasing function $R(r)$ reaches $R(0) \exp(-1)$.

As seen in Tables 1 and 2, our results indicate that the parallel scale lengths are larger than the perpendicular ones for the slow solar wind, and vice versa for the fast solar wind, which is consistent with Figures 1 and 2. Also, note that for the slow wind the anisotropy is more pronounced at smaller scales than at larger scales, something expected from numerical simulation studies and phenomenological arguments (see, e.g., Oughton et al. 1994; Cho & Vishniac 2000; Milano et al. 2001).

From the analysis of 5 years of solar wind data on the Sun–Earth line at 1 AU, we have presented a study of anisotropy in the velocity, magnetic, and cross-helicity fluctuations, as a function of solar wind speed. The source of anisotropy is the "local" mean magnetic field (Milano et al. 2001). Our results show, in all cases, similar anisotropy for the total energy and the cross helicity. We find the appealing result that the fluctuations decorrelate faster in the perpendicular direction in the slow wind and that the opposite occurs in the fast wind.

These results extend and give physical insight into previous results (Matthaeus et al. 1990) that showed distinct lobes aligned with the perpendicular ("slab" population) and parallel ("quasi–two-dimensional" population) axes. The present observations show that the slab lobe corresponds predominantly

to the fast solar wind and the "quasi–two-dimensional" lobe corresponds predominantly to the slow solar wind.

We also computed the spectra (not shown here, for brevity) of the normalized cross helicities $(R_{\mathrm{out}} - R_{\mathrm{in}})/(R_{\mathrm{out}} + R_{\mathrm{in}})$ [$\sigma_c(k)$, often though of as a proxy for the waves' activity; see, e.g., Milano et al. 2004] for both fast and slow winds, averaging all values of θ. In the inertial range we find $\sigma_c(k) \sim 0.7$–0.8 for fast solar wind and $\sigma_c(k) \sim 0.5$–0.6 for the slow one. This confirms, for our ensemble, the result of Marsch & Tu (1990) that the fast wind at a given heliocentric distance shows higher values of inertial range σ_c than does the slow wind at the same distance. This supports the idea of a more turbulent "older" slow wind and a more Alfvénic, "younger" fast wind. At the same time, cross-communication between components makes $\sigma_c(k)$ more or less evenly distributed among different angular directions, consistent with earlier results (Milano et al. 2004).

Here we have focused on the effect of solar wind speed on the type of observed anisotropy. Future studies may further clarify how anisotropy might vary with solar wind composition and magnetic field topology, to study possible differences in plasma from coronal holes, coronal mass ejections, magnetic clouds, and other subcategories of solar wind.

REFERENCES

Belcher, J. W. & Davis, L., Jr. 1971, J. Geophys. Res., 76, 3534
Blackman, R. B., & Tukey, J. W. 1958, Measurements of Power Spectra (Mineola, NY: Dover)
Cho, J., & Vishniac, E. T. 2000, ApJ, 539, 273
Ghosh, S., Matthaeus, W. H., Roberts, D. A., & Goldstein, M. L. 1998a, J. Geophys. Res., 103, 23691
———. 1998b, J. Geophys. Res., 103, 23705
Goldstein, M. L., Roberts, D. A., & Deane, A. 2003, in AIP Conf. Proc. 679, Solar Wind Ten, ed. M. Velli, R. Bruno, & F. Malara (Melville, NY: AIP), 405
Henke, T., et al. 1998, Geophys. Res. Lett., 25, 3465
Marsch, E., & Tu, C.-Y. 1990, J. Geophys. Res., 95, 8211
Matthaeus, W. H., & Goldstein, M. L. 1982, J. Geophys. Res., 87, 6011
Matthaeus, W. H., Goldstein, M. L., & Roberts, D. A. 1990, J. Geophys. Res., 95, 20673
McComas, D. J., Bame, S. J., Barker, P., Feldman, W. C., Phillips, J. L., Riley, P., & Griffee, J. W. 1998, Space Sci. Rev., 86, 563

Milano, L. J., Dasso, S., Matthaeus, W. H., & Smith, C. 2004, Phys. Rev. Lett., 93, 155005
Milano, L. J., Matthaeus, W. H., Dmitruk, P., & Montgomery, D. C. 2001, Phys. Plasmas, 8, 2673
Montgomery, D. C., Liu, C.-S., & Vahala, G. 1972, Phys. Fluids, 15, 815
Oughton, S., Priest, E. R., & Matthaeus, W. H. 1994, J. Fluid Mech., 280, 95
Robinson, D. C., & Rusbridge, M. G. 1971, Phys. Fluids, 14, 2499
Smith, C. W., L'Heureux, J., Ness, N. F., Acuña, M. H., Burlaga, L. F., & Scheifele, J. 1998, Space Sci. Rev., 86, 613
Taylor, G. I. 1938, Proc. R. Soc. London A, 164, 476
Tu, C.-Y., & Marsch, E. 1995, MHD Structures, Waves and Turbulence in the Solar Wind (Dordrecht: Kluwer)
Zhou, Y., Matthaeus, W. H., & Dmitruk, P. 2004, Rev. Mod. Phys., 76, 1015
Zurbuchen, T. H., Fisk, L. A., Gloeckler, G., & von Steiger, R. 2002, Geophys. Res. Lett., 29(9), 1352